Harnessing Demand Flexibility in Electric Distribution Systems

Marie-Louise Arlt
Ludwig Maximilian University/SLAC, marie-louise.arlt@econ.lmu.de

David Chassin
SLAC, dchassin@slac.stanford.edu

Claudio Rivetta
SLAC, rivetta@slac.stanford.edu

James Sweeney
Stanford University, jim.sweeney@stanford.edu

The advent of decentralized renewable energy resources allows distribution systems – the lower voltage levels of the electricity grid – to play an increasingly active role in the efficient operations of power systems. In this work, we suggest an approach to manage load flexibility of customers in residential distribution systems, an under-utilized resource. Specifically, we integrate a market-based coordination mechanism with automated representation of customer preferences by smart home systems to determine the efficient dispatch of appliances in real-time and manage a potential constraint to the overlying grid. For that purpose, we conceptualize how customers' real-time willingness-to-pay for the dispatch of time-interdependent electricity-based services can automatically be derived. We specify our approach for Heating, Ventilation, and Air Conditioning (HVAC) systems and show that customer preferences can be easily provided through an intuitive slider. Finally, we demonstrate the benefits of our approach in a case study of 437 houses in Austin, Texas, and estimate gains of more than 17,000 USD over one year, and significantly more in constrained systems. We find that all customers contribute to the welfare gain and that all customers benefit, although not equally. Moreover, our approach is likely to decrease optimal grid investment. Our work makes important suggestions on how the flexibility potential of residential demand can be unleashed through the means of automation and provides insight into the distribution of welfare gains among heterogeneous customers.

Key words: Residential demand management, smart home systems, automation, distribution systems, local electricity markets

History: First submission on May 1, 2021.

1. Introduction

The advent of decentralized renewable energy resources such as solar energy and new flexible loads such as heat pumps, electric vehicles, or residential battery storage allows distribution systems – the lower voltage levels of the electricity grid – to play an increas-

ingly active role in the efficient operations of power systems. In this work, we suggest an approach to manage load flexibility of customers in residential distribution systems, an under-utilized resource. Specifically, we integrate a market-based coordination mechanism with automated representation of customer preferences by smart home systems to determine the efficient dispatch of appliances in real-time and manage a potential constraint to the overlying grid.

Second, we conceptualize how customers' real-time willingness-to-pay for the dispatch of time-interdependent electricity-based services can automatically be derived and implemented in a smart home system. This is challenging as customers usually only form preferences towards the service provided by an appliance (e.g. temperature control or electric vehicle driving) but not towards the real-time consumption of electricity. We specify our approach for Heating, Ventilation, and Air Conditioning (HVAC) systems, a major residential and potentially flexible load. Our algorithm can be easily deployed in smart home systems: just as under a fixed retail rate, the setup of the HVAC system only requires two distinct inputs by the customer – the comfort temperature and a comfort preference – and we show that these parameters can be easily set through an intuitive slider.

Third, we demonstrate the benefits of our approach in a case study of 437 houses in Austin, Texas, and estimate gains of more than 17,000 USD over one year, and significantly more in constrained systems. We find that all customers contribute to that welfare gain, although not equally, and analyze the distributional effects: customers who contribute more also benefit more and even over-proportionally, and the largest savings go to those who had high electricity bills in the first place. In our case study, high electricity bills are mainly driven by large floor sizes, indicating potential re-distribution effects between high- and low-income customers. Finally, we show that active demand management is likely to decrease optimal grid investment.

Our work contributes to existing efforts to flexibilize demand and enable an efficient dispatch of resources (e.g. Borenstein and Holland 2005, Borenstein 2007, Chen and Gallego 2019) as well as investment (e.g. Borenstein 2007, Kök et al. 2018, Comello and Reichelstein 2019). Tariffs and programs such as Time-of-Use rates, real-time pricing, or critical peak pricing have shown to be generally effective in shaping residential demand (e.g. Allcott 2011, Wolak 2011, Burkhardt et al. 2019). Furthermore, strategies have been developed which address the challenges of residential distribution systems more specifically,

for instance with regard to the cost incentives of municipal utilities or the management of more frequent congestion to the overlying grid (Cohen and Callaway 2016, Cohen et al. 2016, Astier and Rajagopal 2021). Such strategies rely on dynamic pricing (e.g. Adelman and Uçkun 2019, Valogianni et al. 2020), markets (e.g. Hammerstrom 2007, Widergren et al. 2014, Mengelkamp et al. 2018, Liu et al. 2018, Rassa et al. 2019, Ableitner et al. 2020), and centralized coordination of appliances based on technical requirements (e.g. Dimeas and Hatziargyriou 2005, Radovanovic et al. 2016). In our paper, we chose a market-based approach because it allows customers to express their preference for dispatch and does not require access to private information for a centralized optimization.

To our knowledge, the existing approaches to market-based demand management have, however, not developed an integrated framework of how customer preferences can be represented. Manual input of willingness-to-pay can usually only address environments where real-time optimization is not required, for instance because of non-time-dependent supply costs (e.g. Mengelkamp et al. 2018, Wörner et al. 2019, Ableitner et al. 2020). However, with increasing shares of renewable energy and more volatile prices, automation has been recognized as key to access demand flexibility under fast-changing conditions (Faruqui and Sergici 2010, Bollinger and Hartmann 2020). Adelman and Uçkun (2019) present an effective price-based automated control of HVAC systems. Current designs of transactive systems furthermore enable automated bidding based on heuristics, including customer input for comfort preference (e.g. Hammerstrom 2007, Widergren et al. 2014). In contrast, automated dispatch algorithms proposed by the technical literature usually aim to minimize electricity cost, see Lin et al. (2015), Vrettos and Andersson (2016) for HVAC systems or Seddig et al. (2019), Graber et al. (2020) for electric vehicles, but disregard a trade-off with comfort. In our work, we suggest how the real-time willingness-to-pay for time-interdependent electricity-based services can be conceptualized in a consistent economic framework and operationalized in a smart home system.

Furthermore, there is currently only limited literature on how residential demand management affects distribution systems, customers, and the distribution of consumer surplus between them. The literature on wholesale energy markets and transmission systems has broadly discussed the welfare gains enabled by load flexibility (e.g. Borenstein 2005, 2007). The underlying concepts are widely used in practice, e.g. for the evaluation of generation and grid capacity (CAISO 2017, ENTSO-E 2018, CAISO 2020, PJM 2020). However, they

are not directly applicable to distribution systems as they lack the residential customer perspective. For distribution systems, previous work has focused on alternative performance indicators of residential demand management such as self-sufficiency (e.g. Ableitner et al. 2020, Wörner et al. 2019) or successful capacity management in distribution systems (e.g. Hammerstrom 2007, Widergren et al. 2014). Hammerstrom et al. (2016) have proposed a comprehensive valuation framework but have not specified the residential customer perspective nor analyzed consumer surplus changes. Notable exceptions are Adelman and Uçkun (2019) and Bollinger and Hartmann (2020). Adelman and Uçkun (2019) approximate consumer surplus based on a triangular utility function. Bollinger and Hartmann (2020) estimate the welfare change enabled by automation under time-of-use and critical peak pricing, using empirical data. We extend their work by quantifying welfare changes in unconstrained and constrained settings with real-time supply costs, and explore distributional effects among heterogeneous customers.

Our work has important practical implications. Previous work has demonstrated that automation plays a key role in accessing demand flexibility, especially when responding to quickly changing conditions (e.g. Faruqui and Sergici 2010, Bollinger and Hartmann 2020). Our work shows that a real-time demand management system and a well-designed bidding strategy with intuitive customer input can realize substantial benefits. Manufacturers and other relevant providers should work on improved and additional automation strategies for flexible appliances. Burger et al. (2019) have further highlighted that the distributional consequences of time-dependent pricing can be substantial. We provide further evidence on these effects under automation and for HVAC systems which are owned by a large share of the population. Such effects should be closely studied when demand becomes increasingly flexible to accommodate higher shares of renewable energy.

We proceed as follows: In Section 2, we describe our market-based residential demand management system. In Section 3, we characterize the real-time willingness-to-pay for time-interdependent electricity-based services and specify a bidding function for HVAC operations. Section 4 introduces our case study of 437 residential customers in Austin, Texas. We provide our results for customers and the retailer in Section 5. Section 6 concludes this paper by a brief summary, managerial and policy implications, as well as a research outlook.

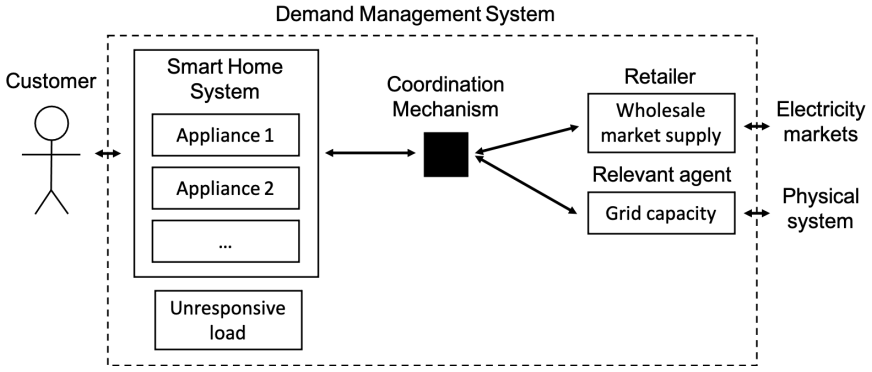

Figure 1 Components of demand management system

2. Demand Management System

Our demand management system consists of several components which are displayed by Fig. 1 and described as follows. The customer i enters his preferences for the dispatch of appliances through the smart home system (e.g. the preferred temperature for an HVAC system or the minimum range for an electric vehicle). At the beginning of each market interval t and separately for each appliance j, the smart home system then combines these preferences with relevant physical information (e.g. the current temperature or state-of-charge of a battery) into a real-time willingness-to-pay b_t^j. In the following Section 3, we will illustrate how such a mapping could be motivated. The willingness-to-pay b_t^j, together with the required power P^j, is submitted to the operator of the demand management system. The bid represents the customer's willingness-to-pay b_t^j for the dispatch of his appliance j at the power P^j over the full duration Δt of the upcoming market interval. Unresponsive load of the customer, e.g. demand for electric lighting, is not managed by the smart home system. Instead, the respective retailer places a bid on behalf of the aggregate of unresponsive loads in the distribution system, including non-bidding appliances as well as grid losses. On the supply side, the retailer offers electricity from the wholesale market at marginal costs of c_t^{WS}, which corresponds to the price of electricity and a mark-up for grid losses.

Once all bids have been submitted, the operator of the demand management system aggregates all demand bids b_t^j in a downward-sloping demand function $D_t(p)$, with $D_t'(p) < 0$, and clears the market for the upcoming market interval by determining the market-clearing price p_t and communicating that price to all automated appliances. The role of the operator can be played by (local) integrated utilities or cooperatives, community choice aggregators, distribution system operators, or a third party provider. Market

clearing is subject to the limited connection to the overlying grid which constrains import from the wholesale market. The information on available grid capacity is provided by the agent operating the grid, i.e. the local utility or a distribution system operator.

The system can take two states: unconstrained and constrained. If $D_t(p = c_t^{WS})$ is less or equal to the import constraint from the transmission system, all demand can be satisfied and the distribution system is unconstrained. Then, the clearing price p_t equals the supply cost from the wholesale market. If, however, $D_t(p = c_t^{WS})$ exceeds the import constraint, not all demand can be satisfied and the system is constrained. As a result, the clearing price p_t increases above the level of the supply costs c_t^{WS} until demand $D_t(p_t)$ is equal to or less than the import constraint.

Based on the published clearing price p_t, smart home systems can infer the dispatch of their appliances. An appliance j is dispatch if $b_t^j \geq p_t$ and is not dispatched if $b_t^j < p_t$. As customers have no advantage in mis-representing their true willingness-to-pay when submitting b_t^j, this dispatch behavior is individually rational and the market result will indeed be implemented. Unresponsive loads are not sensitive to p_t and dispatch as needed. Our demand management system represents a market-based coordination mechanism which allows for the priority-based dispatch of flexible appliances, considering the real-time cost of supply. Future versions of this system could furthermore integrate local generation and storage or consider congestion within the distribution system.

3. Automating Customer Choice

In this section, we describe how the smart home system should represent customer preferences in real-time. First, we characterize the willingness-to-pay for dispatch in a general model of time-interdependent electricity-based services (Section 3.1). Second, we propose a bidding strategy for HVAC systems – a major and potentially flexible load in residential systems (Section 3.2).

3.1. General Characterization of Willingness-to-Pay

Residential distribution systems are dominated by appliances like HVAC systems, water heaters, or electric vehicles which provide time-interdependent services. The dispatch of such appliances is motivated by an inter-temporal utility maximization problem which

trades off the benefits from the service and the cost associated with electricity consumption. For readability, we drop consumer- and appliance-specific indices i and j,

$$\max_{\mathbf{b}} \mathbb{E}\{\sum_{t=0}^{T-1}[u(x_t) - p_t P d_t(b_t)\Delta t] + U_T(x_T)\} \tag{1}$$
$$\text{s.t. } x_{t+1} = f(x_t, d_t(b_t)), \forall t \in \{0, ..., T-1\}$$
$$d_t, x_t \in \mathbf{C}^{load}, \forall t \in \{0, ..., T-1\}.$$

At each stage t of the optimization horizon T, the customer experiences a utility $u(x_t)$ which is a function of the quality x_t of a service provided by an electric appliance. For instance, x_t can reflect the internal temperature of a house (for an HVAC system) or the range available for driving (for the battery of an electric vehicle). The quality of service x_t is usually coupled in time and can be influenced by the discrete dispatch of the respective appliance, i.e. $d_t \in \{0, 1\}$. The dispatch of the appliance is subject to electricity costs which correspond to the product of the energy consumed during the market interval, $P\Delta t d_t$, and the cost of electricity, p_t. We assume that customer utility is linear in money. The dispatch as well as the service quality provided by the electric appliance are subject to a set of constraints $\mathbf{C}^{load}$, for instance the maximum or minimum internal temperature or the minimum mileage of the battery of an electric vehicle at the estimated time of departure. The relationship between dispatch and time-interdependent service quality is described by the transition function $x_{t+1} = f(x_t, d_t)$. $U_T(x_T)$ represents the disposal utility at the end of the optimization horizon.

The customer optimizes his inter-temporal utility by determining his willingness-to-pay for dispatch b_t for submission to the demand management system. Our formulation differs from conventional optimal scheduling problems where p_t is known and the customer decides on d_t directly. To characterize b_t, we take advantage of the value function $V_t(x_t)$. For time t and given the service quality x_t, $V_t(x_t)$ describes the customer's expected value from optimally operating the appliance till the end of the time horizon T.

Definition 1. The willingness-to-pay b_t is defined as the price at which the customer is indifferent between current and future dispatch,

$$b_t = \frac{V_{t+1}(x_{t+1}|d_t = 1) - V_{t+1}(x_{t+1}|d_t = 0)}{P\Delta t}. \tag{2}$$

Symbol	Description	Symbol	Description
General customer model		***HVAC model***	
t	Time index	α	Comfort preference
T	Optimization horizon	θ_t	Internal temperature
$u(\cdot)$	Utility function	θ^{com}	Comfort temperature
$U(\cdot)$	Disposal utility	θ^{out}	Outdoor temperature
b_t	Willingness to pay	β	Thermal house characteristics
x_t	Service quality	m	Operation mode (heating/cooling)
p_t	Local electricity price	γ_m	HVAC efficiency
P	Rated power of appliance		
d_t	Dispatch		
Δt	Market interval		
$f(\cdot)$	Transition function		
$\mathbb{C}^{load}$	Appliance constraints		
$V_t(\cdot)$	Value function		
c_t^{WS}	Wholesale market supply cost		

Table 1 Variables and parameters

Importantly, the willingness-to-pay b_t does not only consider the value from operations in t but also trades off current dispatch with a delayed dispatch in future periods. In particular, b_t depends on future prices $p_{t'}$ in $t' > t$ and, given the same initial state x_t, will be generally lower if low prices are expected, compared to high expected prices. This formulation contrasts other contributions in the field which do not consider demand and, therefore, bids to be time-interdependent (e.g. Borenstein 2005, Baake et al. 2020).

To conclude, we want to further highlight that the willingness-to-pay as characterized here and specified in the following section is not only helpful for our demand management system but can likewise be leveraged in other applications. For instance, it could be locally implemented in a smart home system to automatically respond to real-time prices. Such an implementation could avoid extreme bill increases, as recently observed during the Texas energy crisis (e.g. McDonnell Nieto del Rio et al. 2021). Furthermore, individual benefits from efficient dispatch can already be reaped without the implementation of the centralized coordination mechanism.

3.2. Willingness-to-Pay for HVAC Systems

We now specify the bidding function for HVAC operations to be implemented in the smart home system. For that purpose, we assume that the customer's utility from temperature control can be approximated by a quadratic utility function,

$$u(\theta) = -\alpha(\theta - \theta^{com})^2. \tag{3}$$

Importantly, the customer model should be reasonably chosen to realize a dispatch which satisfies the customer. If this is not achieved, there is a risk that the customer overrides the smart home system and terminates his participation in the demand management system, with potential negative consequences for overall welfare. We think the choice of this customer model is reasonable because of the following characteristics: stage-wise utility ('comfort') is a function of the deviation of the internal temperature θ_t from the optimal comfort temperature θ^{com}. The comfort of a customer reaches its maximum utility level if the deviation is zero, i.e. $\theta_t = \theta^{com}$. We normalize the maximum utility level to zero. The customer's comfort decreases with an increasing deviation of the internal from the comfort temperature, i.e. $\frac{du(\theta_t)}{d|\theta_t - \theta^{com}|} < 0$, and deteriorates more intensively at larger temperature differences, i.e. $\frac{d^2u(\theta_t)}{d|\theta_t - \theta^{com}|^2} < 0$. Comfort is furthermore scaled by the comfort preference $\alpha \in \mathbf{R}^+$ which is customer-specific.

We describe the dynamics of the internal temperature θ_t by the following equation, using a modified version of the transition function proposed by Mathieu et al. (2013),

$$\theta_{t+1} = \beta\theta_t + (1-\beta)\theta^{out} + m\gamma_m P_m \Delta t d_t. \tag{4}$$

β represents the thermal properties of the house. Higher β are associated with larger thermal inertia of the house, e.g. because of better insulation, and slow down the speed of convergence between the outdoor temperature θ^{out} and the internal temperature θ_t. The latter can be controlled through the operation of the HVAC system. For $m = -1$, the HVAC system is in cooling mode and decreases the internal temperature; for $m = 1$, it is in heating mode and increases the internal temperature. γ_m indicates the efficiency of the HVAC system, depending on its operating mode.

Based on the descriptions of the customer model and the thermal model of the house, we can derive the optimal temperature level θ^* for a given constant price level p.

LEMMA 1 **(Optimal Comfort Gap.)**. *The optimal price-dependent comfort gap, i.e. the difference between the internal and the comfort temperature, can be described by,*

$$|\theta^* - \theta^{com}| = \frac{1-\beta}{2\alpha\gamma_m} p. \tag{5}$$

A detailed derivation of this and the following theoretical results can be found in Section A in the appendix.

Our finding shows that the smart home system would implement an internal temperature equal to the comfort temperature if the cost of electricity was zero. The comfort gap widens with increasing costs of electricity. However, due to their on/off characteristics with $d_t \in \{0,1\}$, HVAC systems cannot keep the internal temperature exactly at the optimal level but only *on average* within a cycle. In equilibrium, a cycle consists of a period during which the HVAC system operates and one or multiple periods during which the HVAC does not operate until the initial (less comfortable) temperature is reached again and the cycle re-starts, i.e. $\theta_{t'} = \theta_t$, for $t' > t$. As a result, the temperature oscillates between the initial temperature θ_0 and the temperature in the subsequent period, $\theta_1 = f(\theta_0, d_0 = 1)$. Then, the temperature is effectively controlled around $\overline{\theta}_0 = (\theta_0 + \theta_1)/2$. A dispatch in t would therefore mean to start a new cycle around the temperature $\overline{\theta}_t$. We propose the following utility-maximizing bidding function for dispatch in t and the start of such a new cycle around $\overline{\theta}_t$.

THEOREM 1 **(Willingness-to-Pay.)**. *The customer's willingness-to-pay for dispatch in t is described by,*

$$b_t = \frac{2\alpha\gamma_m}{1-\beta}|\theta^{com} - \overline{\theta}_t|. \tag{6}$$

If $|\theta^{com} - \overline{\theta}_t| \geq |\theta^{com} - \theta^*|$, then, $b_t \geq p$ and the HVAC system bid will get cleared and the appliance dispatched. As a result, the temperature will oscillate around θ^*. Our bidding strategy would also approximately replicate the optimal cycling behavior around a fixed temperature setpoint under a fixed retail time tariff, without a demand management system. The described cycling behavior results in an optimal average dispatch $d \coloneqq \frac{1}{t'-t}\sum_{\tau=t}^{t'-1} d_t$.

THEOREM 2 **(Optimal Average Dispatch.)**. *The optimal average dispatch d is linear in price and can be described by the following function,*

$$d^* = \frac{1-\beta}{\gamma_m P_m \Delta t}|\theta^{com} - \theta^{out}| - \frac{(1-\beta)^2}{2\alpha\gamma_m^2 P_m \Delta t}p. \tag{7}$$

d^* can be interpreted as the share of periods within which the HVAC system is active ('duty cycle') or the probability of dispatch in a certain period. Likewise, across a population of identical customers, d^* represents the expected share of HVAC systems being switched on. The theorem shows that optimal average dispatch – and therefore also the load in the distribution system – increases if the cost of electricity decreases. The duty cycle furthermore increases if the difference between the comfort and the outside temperature is higher (for instance during winter or summer) and the efficiency and rated power of the HVAC system are lower. The effect of the thermal properties of the house β is ambivalent as better insulation requires less dispatch to maintain a certain temperature, on the other hand, dispatch is more valuable as the effect of dispatch holds on over time.

To illustrate the mechanics of the bidding strategy under changing instead of equilibrium conditions, let us now assume that $\overline{\theta}_t = \theta^*$, given a constant expected price level p. If the price level now increases to $p' > p$, the bid of the HVAC system will not get cleared. Then, the internal temperature will further diverge from the comfort temperature until $|\theta^{com} - \overline{\theta}_{t'}| \geq |\theta^{com} - \theta^*(p^{'})|$.

Our results also illustrate the role of the comfort preference α. Eq. (3) indicates that customers with high values of α are more sensitive to temperature changes, i.e. $|\frac{du(\theta_t)}{d|\theta_t - \theta^{com}|}|_{\alpha} > |\frac{du(\theta_t)}{d|\theta_t - \theta^{com}|}|_{\alpha'}$ for $\alpha > \alpha^{'}$. As a result of a generally higher level of bids b_t (according to Theorem 1), customers with a high value of α will observe a smaller comfort gap (see Lemma 1) and a more frequent dispatch of their HVAC system (see Theorem 2). Furthermore, while the house characteristics β and the HVAC system properties P_m and γ_m are fixed in the short-term, the customer can adjust his comfort setting in the smart home system if his comfort preference changes. For instance, in times of absence, α might be very low and adjusted accordingly. In general, for optimal consideration of this trade-off, the customer should enter his true comfort preference to the smart home system and we will demonstrate in Section 4.3 that this value can easily be provided through an intuitive slider.

4. Case Study

In this section, we present the setup of our case study. We detail the compilation of our simulation model (Section 4.1), describe the behavior of the system under a fixed retail rate (Section 4.2), and present the calibration of our customer model (Section 4.3). Finally, we lay out the concept of how we operationalize the demand management system (Section 4.4).

4.1. Simulation Model and Data

We consider a synthetic distribution system in Austin, Texas, with 437 residential households and one connection point to the overlying grid. We characterize the building stock based on US Energy Information Administration (2015) and US Environmental Protection Agency (2001) which provide data on the geography-specific floor area, house weatherization, HVAC system settings and parameters, etc. The base load of houses (non-flexible load) is derived from household data provided by Inc. Pecan Street (2019) for the year 2016. The electric distribution system is represented by the IEEE 123 feeder (IEEE Power Engineering Society 2014). More details on the population of the feeder and the technical characterization of houses are described in Section B in the appendix. The system is exposed to real-time wholesale market prices for which we use data from the Southern Load Zone in Texas, provided by ERCOT for the year 2016 (Ercot 2019, 2020).

4.2. Benchmark Scenario

We now describe the system behavior under a fixed retail rate ('benchmark scenario'). We use the distribution system software GridLAB-D (SLAC 2020) to simulate one year of operations in five minute intervals. HVAC systems dispatch according to their internal control which keeps the internal temperature between the heating and the cooling setpoint. HVAC systems are the dominant electric load and account for 75.5% of total residential electricity consumption in our system. This finding is in line with previous work, e.g. Burkhardt et al. (2019).

First, we analyze the cost structure of energy procurement. The average cost of a MWh imported to the distribution system is 27.01 USD/MWh and varies significantly throughout the year. Average procurement costs are minimal (13 to 15 USD/MWh) during the month of February and reach a maximum in the first week of August, with 68.91 USD/MWh. Maximum real-time prices can even reach a level of 1,772.80 USD/MWh, as on March 31, 2016. Furthermore, weeks exhibit very different levels of price variations, ranging from an unweighted standard deviation of 4.4 USD/MWh to 136.6 USD/MWh. A detailed description can be found in Table 6 in the appendix.

Analyzing the drivers for individual utility bills under a fixed retail rate, we find that 90% of the variance in bills for HVAC operations between customers are explained by the following parameters: bills increase with an increasing floor area (0.072 USD/sqf), decrease

with improving thermal characteristics (-2,886.62 USD), and increase with increasing comfort preference (4.919e+05 $°F^2$). Furthermore, electricity bills are on average 44.09 USD less for houses which run on gas for heating. The analysis is made under the assumption that the fixed retail rate of the benchmark scenario is determined as the ratio between overall energy procurement cost (including losses) and the energy consumed as measured at customers' meters. As a result, profits for the retailer are zero. The summary of the regression results can be found in Table 7 in the appendix.

Finally, aggregate system load is generally higher for the middle of the summer and the middle of the winter which is driven by electricity consumption of HVAC systems during hot and cold temperatures. In the summer months, system load is higher during the day. It reaches its maximum around 3 to 5pm and decreases afterwards. In contrast, in the winter months, average system load reaches its maximum between 7 and 9 am. The maximum of the system load is 2.311 MW. In 1% of the time, the load is equal or higher than 2.124 MW (91.9% of peak load) and, in 5% of the time, 1.723 MW (74.6%), respectively. This indicates that the system peak load and required import capacity are only driven by a few days within a year. The complete load duration curve as well as weekly maximum load can be found in the appendix, see Fig. 10 and Table 6.

4.3. Calibration of Customer Model

Based on the benchmark scenario, we can now parametrize our customer model as established in Section 3.2. As, in the context of our case study, building parameters as well as comfort preferences can change due to unobserved characteristics such as humidity or solar radiation, we estimate all parameters separately for each week. We first leverage the temperature time series to estimate house-specific parameters β, γ_m, and P_m of Eq. (4), using linear regression. We further determine the comfort preference α and the comfort temperature θ^{com} using the principle of revealed preferences, i.e. we calibrate the utility function of each customer to reproduce the given temperature setpoints under the week-specific fixed retail rate.

Fig. 2a shows the resulting mapping between the temperature range (i.e. the difference between the cooling and the heating setpoints) in the benchmark scenario and the estimated comfort preference α under our demand management system. Customers who provided a narrow temperature band in the fixed retail rate scenario are optimally participating in the demand management system based on a higher comfort preference α. As

customers are unlikely to have a specific understanding of their comfort preference α in numerical terms, the customer could provide it using a slider as displayed in Fig. 2b. Such a slider would represent the trade-off between comfort and costs and can be intuitively set by the customer. Importantly, the participation in our demand management system does not require more information on the side of the customer than under a fixed retail rate. Instead of separate heating and cooling setpoints, the customer would be required to provide his comfort temperature and the comfort preference.

Figure 2 Mapping of comfort preference α to temperature setpoint spread under a fixed retail rate (August 1 - 7, 2016)

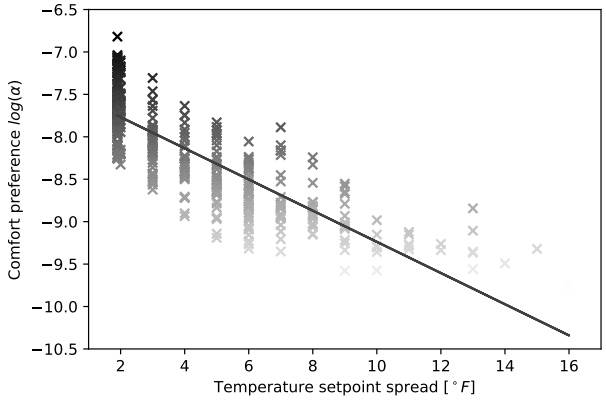

(a) Translation of temperature setpoints into comfort preference

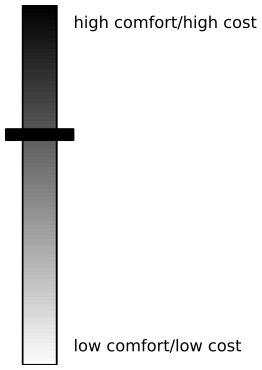

(b) Slider for comfort setting

4.4. Demand Management Scenario

At the beginning of each market interval, the operator of the demand management system collects the bids of HVAC customers. These consist of the willingness-to-pay b_t and the expected required power P_m over the upcoming interval Δt. We approximate P_m by the power which was needed when the appliance was last active in the given mode m. When aggregating the demand curve $D_t(p)$ as described in Section 2, the operator further includes the retailer's bid for unresponsive load which covers appliances not participating in the demand management system as well as grid losses. Again, we use the amount of unresponsive load in the previous period as an estimate for the upcoming period. On the supply side, the supply cost c_t^{WS} from the wholesale market corresponds to the real-time price and a mark-up. This mark-up accounts for grid losses and is calculated based on the

benchmark scenario. The system is run every five minutes and determines the dispatch throughout the upcoming five-minute market interval (Δt). This is a reasonable time interval during which HVAC systems can work efficiently: in a calibration study with timesteps of one minute, the minimum run time of an HVAC system is three minutes and the average duration of consecutive dispatch is 5.6 min.

5. Results

Using the case study introduced in Section 4, we quantify the general welfare effects of our demand management system in Section 5.1. Then, we analyze the implications on customers and the retailer in Section 5.2 and Section 5.3, respectively.

5.1. General Welfare Effects

We calculate welfare changes as the sum of comfort changes for customers, energy procurement cost savings, and avoided congestion costs. This perspective does not require any assumptions about the distribution of welfare gains between customers and the retailer.

Unconstrained system. First, we consider the case of an unconstrained system, i.e. import is unlimited. In that case, no congestion costs apply. We find that, over the course of the year 2016, welfare gains of operating an HVAC system add up to 17,043 USD. Fig. 3a shows realized welfare changes for the 51 full weeks of the year 2016 and their dependence on the standard deviation of the wholesale market price, weighted by system load. This figure allows for two important insights. First, we find that, in most weeks, the system experiences significant positive welfare changes, reaching up to 1,918 USD within a week. There are two weeks for which the welfare change is slightly negative, adding up to a loss of 64 USD. We attribute this finding to an imperfect description of the thermal dynamics of the system by the linear model and the myopic forecasting approach for external parameters. Second, the weighted standard deviation of the wholesale market price within a week is positively correlated with the achievable welfare change, by a coefficient of 0.85. With the standard deviation increasing by 1 USD/MWh, the prospective weekly welfare gain from switching from a fixed retail tariff to our demand management system increases by 11.00 USD.

Fig. 3b furthermore illustrates the cumulative distribution function of welfare gains over households, sorted from the house contributing the most to the one contributing the least to the overall welfare gain. The dashed line benchmarks our empirical finding with a hypothetical uniform distribution of welfare contributions. We find that all houses

Figure 3 Distribution of welfare changes

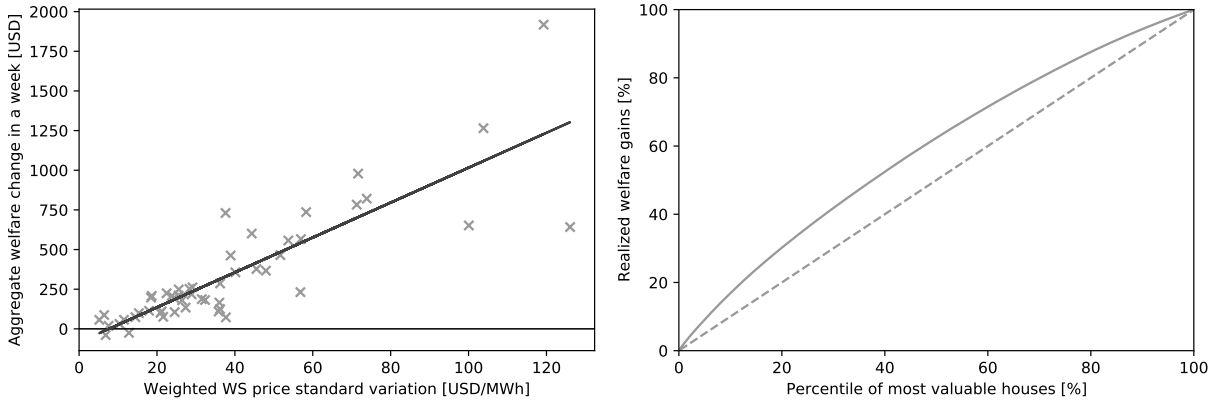

(a) Weekly welfare changes by weighted price standard deviation

(b) Cumulative welfare gain distribution over households

contribute positively to welfare and, thus, should all be considered for participation in the demand management system. However, houses do not contribute equally to the welfare gain but, for instance, the 50% most valuable ones realize already 62.3% of possible welfare gains. The most valuable household contributes 92.86 USD while the least one contributes 18.53 USD.

Constrained system. We further analyze the implications of a demand management system in a constrained system. Fig. 4a demonstrates the ability of the system to integrate a capacity constraint for the peak day of the year, December 19, 2016. Under a fixed retail rate, the aggregated system load (solid light grey line) reaches the peak of 2.311 MW in the early morning hours, driven by electric heating. With the help of a demand management system, however, aggregate system load (dark grey solid line) can successfully be controlled around an exemplary capacity limit of 1.8 MW (dotted line). This is achieved by an increase in the local price. When there is no congestion, the local price equals the wholesale market price plus the mark-up for losses (1.69 USD/MWh). However, if the import constraint binds, the local price (dashed dark grey line) deviates from the real-time price of the wholesale market (dashed light grey line) by up to 20.76 USD/MWh. Local demand is reduced at the higher equilibrium price to equal import-constrained supply, especially during the morning hours until approximately 11am.

Fig. 4b further demonstrates how the load duration curve changes under different capacity constraints. Without our demand management system, the maximum load equals the

Figure 4 Implications of an import constraint (December 19 - 25, 2016)

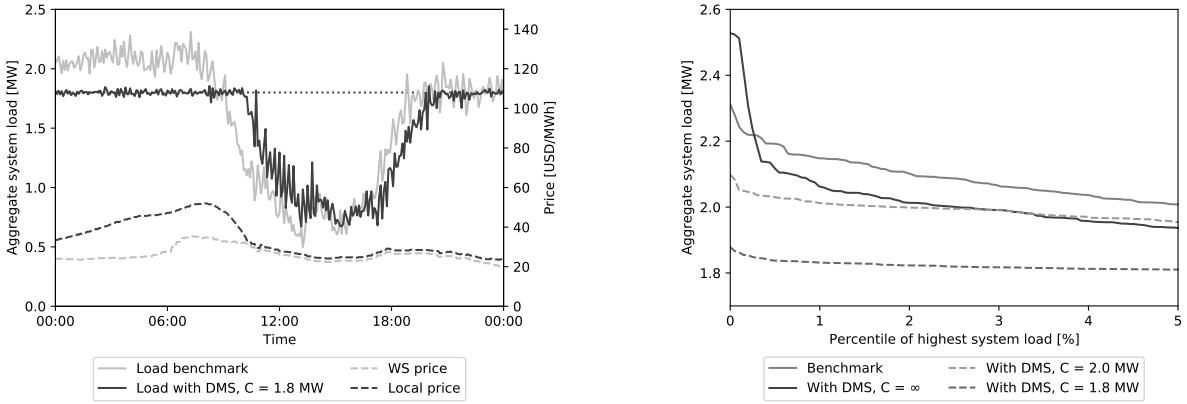

(a) Aggregated load on peak day 12/19/2016 with and without system constraint

(b) Load curves under different scenarios for 5% quantile

year-long maximum of 2.3 MW. If a demand management system is deployed without a capacity constraint, however, the peak system load increases to 2.5 MW. The reason is that low prices and especially sudden price drops can lead to a simultaneous dispatch of many HVAC systems. While this is individually rational and decreases the cost of energy procurement, sudden load increases can be problematic from a system operations perspective (Parag and Sovacool 2016). If a binding capacity constraint is imposed, aggregate load can generally be effectively controlled and decreased (here displayed for system constraints of 2.0 MW and 1.8 MW). It is notable that the aggregate system load can be nearly but not entirely reduced below the capacity constraint. There are multiple reasons for that. First, the system operator makes forecasting errors with regard to the unresponsive load. If the unresponsive load is under-estimated, too much capacity will be allocated to the flexible load and the resulting aggregate system load will exceed the capacity constraint. The maximum forecasting error is 141 kW. Second, the bids submitted might not correspond to the actual consumption of households. For instance, the power drawn by appliances can deviate from their rated power, depending on the grid conditions and other characteristics of the environment such as the outdoor temperature or the voltage quality in the system. Across market intervals, the maximum aggregate deviation caused by HVAC systems not complying with their bids is 25 kW. The error introduced by these two channels are detailed in the appendix, see Fig. 11a and Fig. 11b. Third, system load can be too high if unresponsive load alone exceeds the capacity constraint.

Figure 5 Welfare effects of introducing a demand management system in a constrained system, example of the peak week (December 19 - 25, 2016)

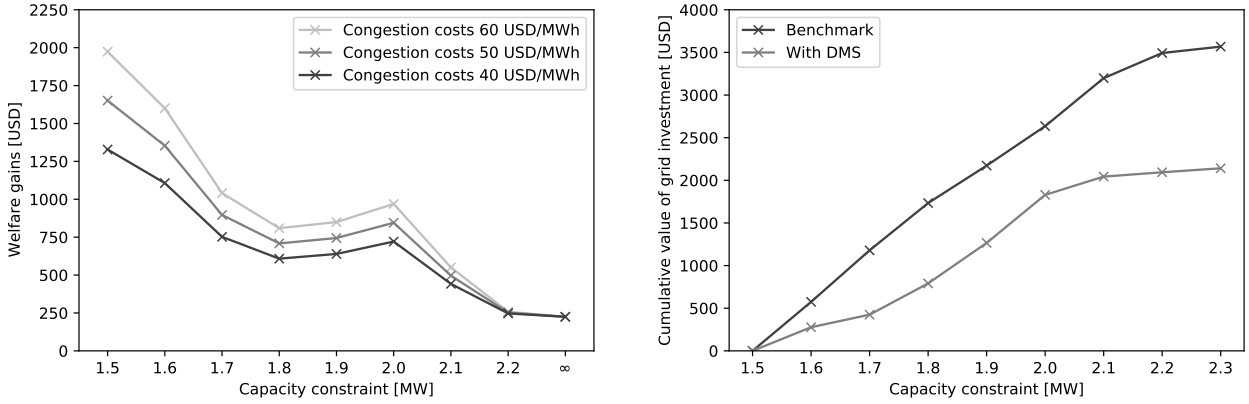

(a) For a given constraint

(b) Compared to a constraint of 1.5 MW

Violating capacity limits can come at considerable cost, e.g. through the degradation of grid components or because of the dispatch of expensive reserve capacity (e.g. diesel generators). We calculate these costs by multiplying the energy consumed by excess load with an estimate for per-unit congestion costs. In our analysis, we apply default cost of 50 USD/MWh which, for instance, corresponds to the marginal cost of operating a diesel generator. For the peak load week of December 19 - 25, 2016, congestion costs can add up to 3,568 USD if the system is constrained to 1.5 MW (the tightest system constraint included in this analysis). In that case, if our system is deployed, significant savings of 1,651 USD can be realized through its capability to manage load. Fig. 5a illustrates these savings for different capacity constraints and congestion costs. We find that the advantage of our demand management system over a fixed retail rate is generally higher for more constrained systems and higher per-unit congestion costs.

According to Joskow and Tirole (2005), efficient investment in the grid infrastructure is the result of a trade off between short-term costs of congestion and long-term costs of grid investment. Fig. 5b provides an insight on the value of grid investment, using the peak load week of December 19 - 25, 2016 as an example. The value of grid investment is calculated as the difference between welfare under the new constraint (enabled by investment) and welfare under a constraint of 1.5 MW. We observe the following facts: first, relaxing import constraints increases welfare but less so if demand is managed. This indicates that, under demand management, less grid investment will be optimal than under a fixed

retail rate, decreasing investment costs in the long-run. Considering the NPV estimate of 700 USD/kWh saved during the peak for delayed investment, as suggested by Bollinger and Hartmann (2020), savings could add up to to 357,700 USD (for a moderate reduction of the peak to 1.8 MW). Second, the marginal value of investment is not monotonously decreasing. In the benchmark scenario, it is highest between 2.0 and 2.1 MW and, with demand management, between 1.9 and 2.0 MW. This indicates that relaxing some levels of constraints can be particularly valuable and adds another layer of complexity to the optimal grid investment problem (e.g. Joskow and Tirole 2005, Lohmann and Rebennack 2017).

5.2. Implications for Customers

The introduction of our demand management system impacts customers in two ways: through changes in comfort as well as their monthly bills. We will first discuss each of these components separately and then consolidate our findings in a combined analysis of consumer surplus.

Comfort. Our evaluation framework allows to quantify the welfare changes associated with temperature variations induced by the demand management system. We find that the mean comfort change across households and throughout the year 2016 is -2.62 USD, with the maximum comfort increase of 17.88 USD and a maximum decrease of 26.75 USD. Furthermore, customers with low comfort preference tend to experience comfort increases while those with high comfort preferences experience comfort losses. Fig. 12a and Fig. 12b provide more detailed evidence in the appendix.

We furthermore provide a detailed analysis of the internal temperature as the driver for comfort changes. As operating modes (i.e. heating/cooling) change between seasons, we focus on the first week of August (week 31) which requires frequent HVAC operations because of high outside temperatures and exhibits the highest average procurement costs (and, therefore, potential savings). We find that, under a fixed retail rate, customers' average internal temperature differs from their comfort temperature by $1.7°F$ ('average comfort gap'). The average comfort gap is larger than zero as the cost of electricity is positive (see Lemma 1). Under a demand management system, this gap reduces to $1.4°F$ on average which corresponds to a decrease in the average comfort gap by 18.0%.

Fig. 6a shows the dependence of the comfort gap change on the comfort preference of customers, aggregated by comfort preference classes of size $\Delta log(\widehat{\alpha}) = 0.5$ (e.g., $log(\widehat{\alpha}) = -8.0$

Figure 6 Temperature as a function of comfort preference α (August 1 - 7, 2016)

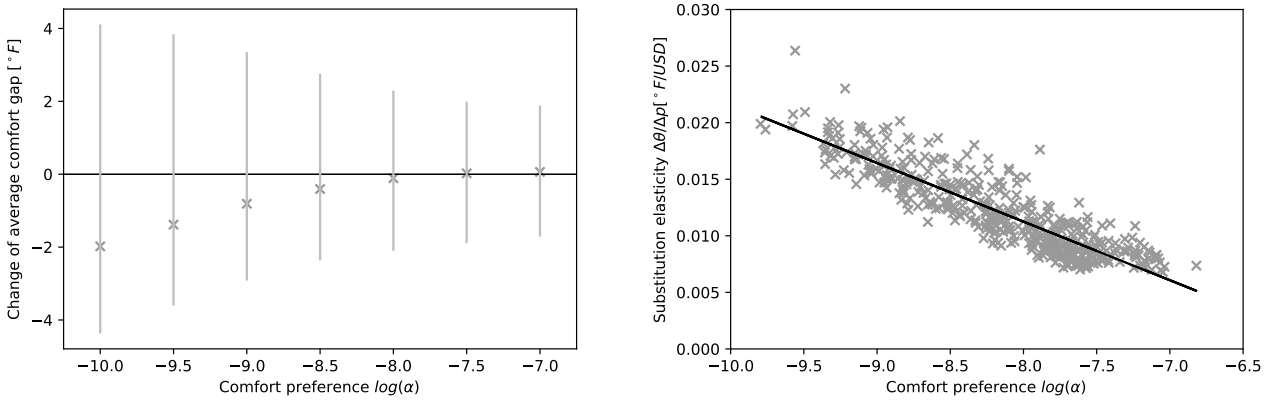

(a) Average comfort gap and temperature spread

(b) Substitution effect between temperature and cost

covers $log(\alpha) \in [-8.25, -7.75[)$. We find that the customers of the lowest comfort preference experience the largest reduction in the average comfort gap (-2.0°F) while customers with the highest comfort preference hardly experience changes in their comfort gap (+0.1°F). The reason is that customers with low comfort preferences react particularly sensitive to price changes and, accordingly, adjust their comfort when local prices drop below the level of the fixed retail rate. This indicates that many periods with low prices allow for a more comfortable dispatch of the HVAC system than in the benchmark case where the relatively high constant retail rate is driven by few high-price periods. However, customers with low comfort preference also react particularly sensitive to high prices. As a consequence, customers with a low comfort preference α experience higher temperature variations. The bars of Fig. 6a represent the temperature spread which is defined as the difference of the 95% and the 5% quantiles of the temperature distribution. We find that, for customers with the lowest comfort preference, the temperature can oscillate up to 6.1°F above and 2.4°F below the comfort temperature. For customers with high comfort preference, this spread reduces to +1.8°F and -1.8°F. In general, the temperature range under our demand management system is higher than under a fixed retail tariff and increases from 3.0°F to 4.8°F, averaged over all customers.

Bill changes. The exact bill changes generally depend on how savings will get re-distributed to customers. For the further analysis, we will assume that appliances participating in the demand management system pay the local price (including the mark-up) and

all other load is billed by a re-calculated retail rate. Savings are not partially retained by the retailer but are fully re-distributed. We find that customers benefit from substantial bill savings. If the system is unconstrained, customers save 18,188 USD which corresponds to 41.62 USD per customer or 14.5%. These bill changes are driven by more cost-effective operations of HVAC systems which contribute 15,660 USD in savings. Moreover, the retail rate for unresponsive loads decreases and enables additional savings of 2,528 USD. The maximum total bill reduction per household is 140.36 USD, the minimum bill reduction 7.15 USD. The maximum relative bill saving per household is 21.4%, the minimum relative bill saving 8.6%.

We furthermore provide an analysis of which customers profit the most. We find that house-specific absolute bill savings can largely be predicted by electricity bills in the benchmark scenario (79% of variance), as described in Section 4.2. Second, savings increase with the share of unresponsive load as of total load, as a result of the decrease in the fixed retail rate. Furthermore, savings are less for customers with a higher correlation of HVAC operations under a fixed retail rate and the wholesale market price, as well as for those with gas heating. More details can be found in Table 8 in the appendix. Similar observations can be made for relative bill savings.

Total welfare. Final consumer surplus is a combination of the changes in comfort and bills. Fig. 6b visualizes the empirical substitution effect between cost and comfort. Customers with a low comfort preference are willing to accept a temperature increase by up to 0.02 $^\circ F$ if the electricity price increases by 1 USD/MWh. Customers with a high comfort preference only accept one fourth, on average. Fig. 7a shows the resulting distribution of house-specific consumer surplus changes. We find that consumer surplus increases consistently for all customers. The average surplus change is 39.00 USD, with a maximum of 118.46 USD and a minimum of 5.50 USD. Further details can be found in the appendix, see Fig. 13.

Finally, we investigate to which extent consumer surplus gains of houses coincide with their welfare contribution to the system, see Fig. 7b. We find that customers who contribute more to system welfare also experience higher consumer surplus gains. This means that the most valuable customers also have a strong private incentive to join the demand management system. However, we also observe that the most valuable customers experience an over-proportional gain in consumer surplus. Summarizing this and previous findings, consumer surplus gains are higher for customers with large floor sizes and such customers

Figure 7 Distribution of consumer surplus changes of houses

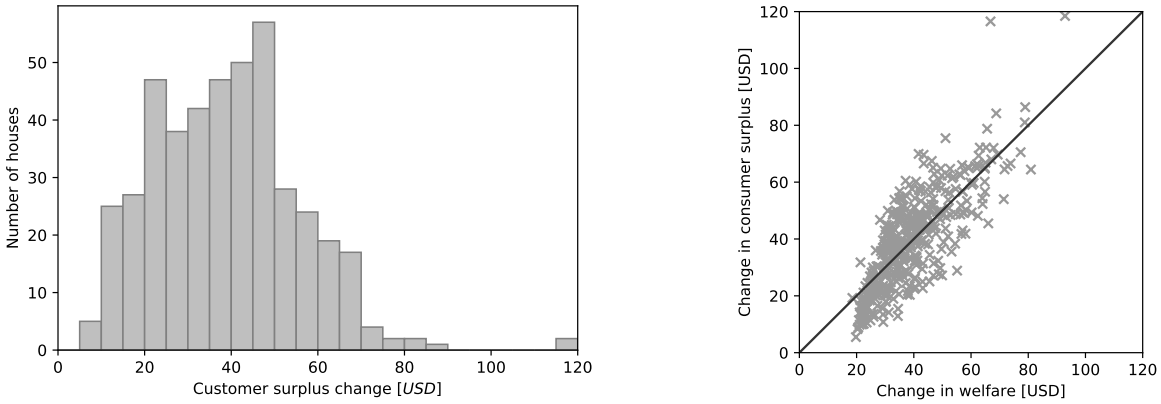

(a) Throughout the year

(b) Consumer surplus gains versus system welfare contribution

	No DMS	DMS
Energy procured [MWh]	4,608	4,717
Share of flexible load [%]	0.00	75.44
Procurement cost [USD]	125,063	106,851
Share of flexible procurement cost [%]	0.00	70.66
Average procurement price [USD/MWh]	27.14	22.66
Fixed retail rate [USD/kWh]	0.027	0.007
Total peak load [MW]	2.311	2.928

Table 2 Key measures of retail business with and without demand management system

benefit over-proportionally compared to their individual contribution to welfare. This may indicate potential re-distribution effects between high- and low-income customers.

5.3. Implications for Retailer

In the following, we analyze how the situation of the retailer changes if a demand management system is deployed. Table 2 summarizes the most important facts for an unconstrained system. We find that the amount of electricity imported by the retailer increases slightly (by 2.4%). However, thanks to the fact that 75.4% of the consumption is price-responsive, energy procurement costs can be decreased by 14.6%. The flexible load requires only an under-proportional share of procurement costs of 70.7% but also unresponsive loads benefit through a fixed retail rate which decreases by 75.5%, from 2.71 ct/kWh to 0.65 ct/kWh. Eventually, we find that the peak load increases by 26.7%, caused by the synchronization of HVAC systems by the price.

We finally investigate the market income, i.e. the income from importing at the wholesale market and re-selling at the local price. For that purpose, we analyze the market income

Capacity constraint [MW]	Market income [USD]
∞	0.00
2.2	3.03
2.1	4.35
2.0	8.92
1.9	96.20
1.8	362.29
1.7	848.95
1.6	1,439.96
1.5	2,084.60

Table 3 Market income under different capacity constraints for December 19 - 25, 2016

for the peak week of the year (December 19 - 25, 2016) under different constraints, as documented by Table 3. If no constraint applies, the market income from congestion is 0 USD. However, with the constraint of the grid being increasingly tight, the market income increases to more than 2,000 USD. This might create an incentive to withhold import capacity. As explained for Fig. 5b, the market income should ideally be invested in grid expansion. However, if the role of the market operator is incorporated by the same entity which is responsible for grid enhancements, this might create an incentive to delay or under-size investment in the grid. Careful regulation can help to address a potential misalignment of incentives.

6. Conclusion and Discussion

In this paper, we suggested a market-based concept to manage residential distribution systems with a constrained connection to the overlying grid. Our system enables the efficient dispatch of customer appliances and management of an import constraint. It can be operated by (local) integrated utilities or cooperatives, community choice aggregators, distribution system operators, or a third party provider. We further propose an approach to automatically derive the willingness-to-pay for the dispatch of time-interdependent electricity-based services such as temperature control, closing the gap between customer preferences for a service and the real-time willingness-to-pay for electricity consumption. This willingness-to-pay cannot only be used in a demand management system as described by us but also in other applications benefiting from automation, such as real-time pricing. We deploy our approach in a case study of 437 houses with HVAC systems in Austin, Texas, and find that welfare gains of more than 17,000 USD can be realized. Additional savings apply in constrained systems and it is likely that less grid expansion is necessary than under a fixed retail rate. We furthermore find that all customers contribute to the

welfare gain and that all customers benefit from a participation in the system, although not equally and with customers with large savings benefiting over-proportionally. Finally, we demonstrate that the operator of our demand management system may face incentives to under-state available capacity or under-invest into the grid.

Our work contributes to the literature on the real-time management of electric distribution systems and the relevance of automation in marketing flexible demand (e.g. Widergren et al. 2014, Adelman and Uçkun 2019, Bollinger and Hartmann 2020). We extend their work in the following ways: first, we suggest how heterogeneous customer preferences can be easily provided to smart home systems and converted to real-time willingness-to-pay. Future work should experimentally validate our proposal and develop concepts for other services, e.g. electric vehicles, to advance our understanding of the interactions between human behavior, technology, and markets (Chen et al. 2020). Second, we provide detailed insights on how automation impacts customers with different comfort-cost trade-offs and house characteristics like the floor area, which are likely to be correlated with socio-economic indicators such as income. In the spirit of Burger et al. (2019), future work should advance the understanding on how automation affects different groups of customers and develop concepts which enable a fair distribution of the cost and benefits. We hope that an improved design of customer-friendly automation strategies and a better understanding of the potentials in residential distribution systems will facilitate a more efficient management of power systems, without compromising acceptance for dynamic incentives and enabling technologies.

Appendix A: Derivation of HVAC Bidding Function

To derive the willingness-to-pay, we take advantage of two characteristics specific to HVAC systems. First, HVAC system usually dispatch multiple times per hour and the typical optimization horizon T is relatively short. Therefore, it is reasonable to assume myopic customer expectations with regard to future prices and outside temperatures. This assumption is also in line with the fact that customers typically do not have access to sophisticated forecasts. Second, due to their on/off characteristics, HVAC systems cannot keep the internal temperature exactly at the optimal level but only *on average*. Therefore, HVAC operations are best described in terms of average dispatch $d := \frac{1}{t'-t}\sum_{\tau=t}^{t'-1} d_t$, with $t' > t$, for which $\theta_{t'} = \theta_t$.

Given stochastic dispatch, we can re-write the transition function Eq. (4) for the expected internal temperature as follows,

$$\mathbb{E}\,\theta_{t+1} = \beta\,\mathbb{E}\,\theta_t + (1-\beta)\theta^{out} + m\gamma_m P_m \Delta t d. \tag{8}$$

Consequently, we can re-write Eq. (8) using $\mathbb{E}\,\theta_t = \mathbb{E}\,\theta_{t+1} = \theta$ to describe the relationship between the average temperature θ and the average dispatch d,

$$\theta = \theta^{out} + \frac{m\gamma_m P_m \Delta t}{1-\beta} d. \tag{9}$$

Given the cycling behavior of HVAC systems, we now re-write the inter-temporal optimization problem of Eq. (1) as a function of average dispatch,

$$\max_d u(\theta(d)) - pP_m d\Delta t. \tag{10}$$

Inserting Eq. (9) and taking the first derivative with respect to d, we can solve for the optimal average dispatch d^* as described by Theorem 2, given the expected constant price level p over the optimization horizon. Inserting into Eq. (9) further allows to derive the optimal temperature level θ^*, as described in Lemma 1.

Appendix B: Data and Feeder Assembly

House data. We generate houses based on survey data provided by US Energy Information Administration (2015). For each house, we randomly draw the number of stories (one or two) and the floor area according to the mean and standard deviation provided. With regard to the thermal system, we consider the most important technologies: resistive heating, heat pump, and natural gas (for heating) as well as electric cooling with or without a heat pump (for cooling). For each feasible combination, the probabilities for a house operating a certain type of HVAC system as well as heating and cooling setpoints are estimated based on the data for the West South Central CENSUS region provided by the US Energy Information Administration (2015). For the other technical characteristics, we use the recommendations for default parameters as provided by GridLAB-D (SLAC 2020). Table 4 and Table 5 summarize the parameters. Furthermore, we calculate natural air changes by hour for one and two story buildings in Zone 2 under normal conditions, using the ACH_{50} value specific to climate zone 2A and the LBL factor provided by US Environmental Protection Agency (2001). Residential base load follows smart meter data published by the Pecan Street data project (Inc. Pecan Street 2019). We use a subset containing all data from Austin for the year 2016 because the number of distinct base load profiles is highest (108).

Parameter	**Average Value**	**Standard Deviation**	**Share** [%]
Floor size $[ft^2]$			
- 1 story	1976.96	47.05	72.09
- 2 stories	3202.38	226.41	27.91
Heating [%]			
- resistive			49.60
- heat pump			8.80
- natural gas			41.60
Cooling [%]			
- heat pump			83.04
- electric, no heat pump			16.07
Setpoints $[^\circ F]$			
- heating	70.77	2.93	
- cooling	73.70	3.33	

Table 4 Parametrization of detached single-family houses (West South Central) (US Energy Information Administration 2015)

HVAC System	1 story	2 stories
Electric cooling / NG heating	24.90%	9.64%
Electric cooling / resistive heating	29.69%	11.49%
Heat pump	17.50%	6.77%

Table 5 HVAC system statistics for housing types (US Energy Information Administration 2015)

Feeder. We model the physical network using the IEEE 123 feeder which represents a typical residential distribution grid. The feeder has a single connection to the overlying grid. The feeder branches out into multiple sub-feeders, representing streets. A graphical illustration of the feeder is displayed by Fig. 8. We further established a routine to populate the feeder to build an electrically balanced distribution system. We accommodate 2,000 detached single-family houses for an initial hosting capacity analysis. Houses are randomly generated according to the data provided at the beginning of this section. We simulate electric load for the month of July, using GridLAB-D (SLAC 2020). We determine the average power per house at the time of maximum load, the After Diversity Maximum Demand (ADMD) factor, which is 4.59 kW. In a second step, we use this factor to randomly assign houses to nodes of the IEEE123 feeder while respecting the maximum hosting capacity of each node. The latter is provided by the specifications of the IEEE123 model (IEEE Power Engineering Society 2014). We determine the design capacity by multiplying this value with a safety factor of 0.66 and iteratively assign houses to nodes until none of the nodes is able to accommodate more load of the size described by the ADMD anymore. We find that 437 houses in total can be accommodated. The maximum hosting capacity is 3.6 MW.

Price data. We use Ercot price data. Austin is part of the Southern Hub (Ercot 2018) and we use the historical price data for 2016 which is available for the Southern Hub in 15 minute intervals for the Real-Time market (Ercot 2019).

Weather data. We use tmy3 data (722540TYA) for Austin (NREL 2015) which represents hourly local median weather conditions, including temperature, solar radiation, and wind speed.

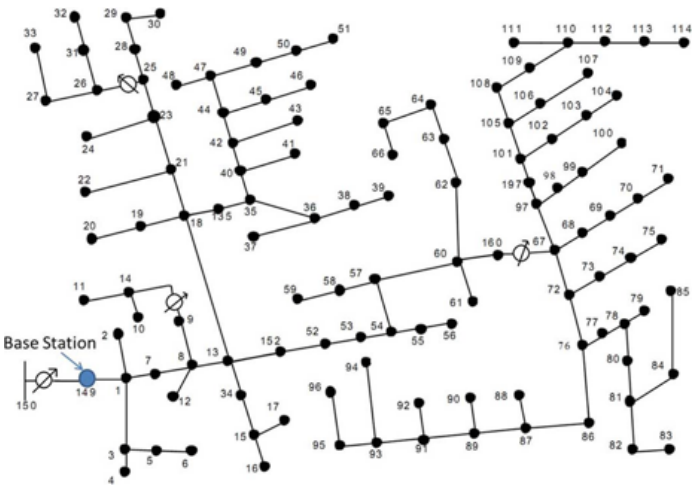

Figure 8 **IEEE 123 feeder (IEEE Power Engineering Society 2014)**

Appendix C: Detailed Results for Base Case

Week	**Av. procurement cost** $[USD/MWh]$	**Max. price** $[USD/MWh]$	**Standard deviation price** $[USD/MWh]$	**Max. load** $[MW]$
01/04 - 01/10	20.76	639.13	26.023	2.116
01/11 - 01/17	17.03	355.41	24.656	1.539
01/18 - 01/24	17.73	340.31	14.373	2.260
01/25 - 01/31	21.87	306.75	42.504	1.802
02/01 - 02/07	13.45	61.67	4.387	1.818
02/08 - 02/14	14.71	108.95	6.675	1.453
02/15 - 02/21	14.53	363.37	26.223	1.441
02/22 - 02/28	14.65	972.00	45.911	1.462
02/29 - 03/06	14.70	360.59	28.310	1.316
03/07 - 03/13	23.25	538.92	50.576	1.731
03/14 - 03/20	33.40	277.84	38.529	1.281
03/21 - 03/27	20.43	799.56	44.566	0.995
03/28 - 04/03	26.73	1772.80	136.637	1.430
04/04 - 04/10	17.47	350.21	20.482	1.241
04/11 - 04/17	19.48	211.40	16.814	1.484
04/18 - 04/24	32.33	235.26	28.651	1.369
04/25 - 05/01	32.79	1507.76	72.479	1.348
05/02 - 05/08	18.95	500.21	28.521	1.244
05/09 - 05/15	29.81	638.87	34.401	1.346
05/16 - 05/22	30.88	860.73	61.269	1.615
05/23 - 05/29	27.30	415.24	29.861	1.471
05/30 - 06/05	21.23	165.89	9.796	1.454
06/06 - 06/12	26.83	338.21	20.587	1.714
06/13 - 06/19	27.97	214.30	13.541	1.599
06/20 - 06/26	25.14	163.41	8.543	1.622
06/27 - 07/03	33.72	548.80	28.132	1.523
07/04 - 07/10	26.97	183.80	12.440	1.684
07/11 - 07/17	28.81	397.44	21.364	1.652
07/18 - 07/24	46.52	665.79	50.329	2.079

Week	Av. procurement cost $[USD/MWh]$	Max. price $[USD/MWh]$	Standard deviation price $[USD/MWh]$	Max. load $[MW]$
07/25 - 07/31	34.72	693.30	38.253	1.659
08/01 - 08/07	68.91	899.52	86.736	1.674
08/08 - 08/14	34.30	221.10	15.130	1.621
08/15 - 08/21	25.08	313.94	18.239	1.751
08/22 - 08/28	34.16	377.76	30.518	1.698
08/29 - 09/04	26.34	64.64	5.753	1.536
09/05 - 09/11	29.20	297.98	20.420	1.514
09/12 - 09/18	55.08	871.30	71.342	1.383
09/19 - 09/25	35.22	417.36	26.327	1.231
09/26 - 10/02	31.32	319.19	21.474	1.421
10/03 - 10/09	48.31	734.63	46.305	1.448
10/10 - 10/16	27.75	329.99	14.999	1.316
10/17 - 10/23	24.96	749.98	35.899	0.985
10/24 - 10/30	28.77	443.80	24.266	1.123
10/31 - 11/06	23.81	379.71	17.515	1.257
11/07 - 11/13	17.50	271.73	11.926	1.246
11/14 - 11/20	18.87	450.85	22.181	0.958
11/21 - 11/27	20.70	340.64	24.628	1.176
11/28 - 12/04	28.19	812.22	72.477	1.654
12/05 - 12/11	24.75	504.45	30.528	1.501
12/12 - 12/18	20.78	505.19	23.617	2.194
12/19 - 12/25	21.22	398.08	24.170	2.311

Table 6: Load and price summary for each week of the year 2016

Table 6 presents key figures for each week of the simulation year 2016. The first three columns provide information on the energy procurement cost. The average procurement cost describes the weighted average price which the retailer pays for each unit of energy $[MWh]$ imported from the wholesale market. The maximum price corresponds to the maximum real-time price on the wholesale market during this week. The standard deviation of the wholesale market price reflects the price variability during the week. The last column provides the maximum feeder load, measured at the connection point to the aggregate system level. The feeder load is important for the sizing of the transformer at the connection to the aggregate system level and a relevant cost driver.

Fig. 9 shows the resulting average system load for each hour of the day in each month of the year, as measured at the point of connection to the aggregate system level. Summer months are depicted in dark colours, winter months in light colours. We use dashed lines to represent the months of the first half of the year and solid lines for the months of the second half.

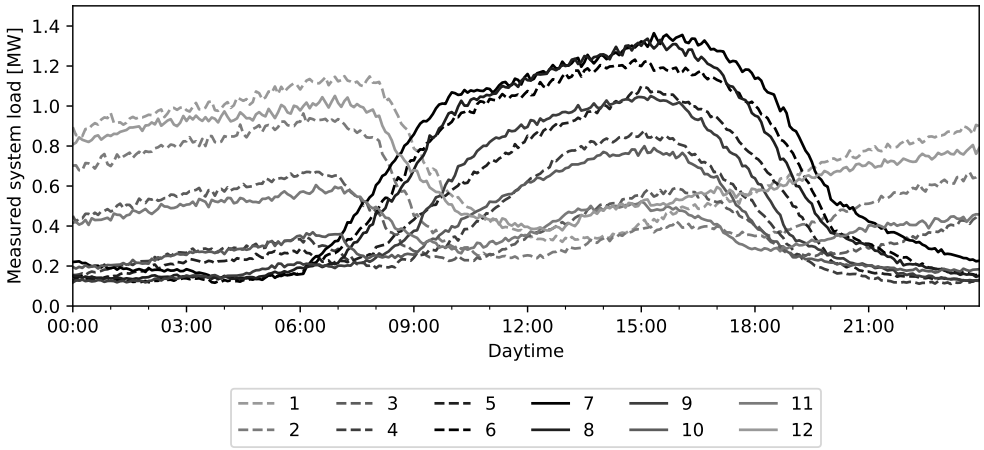

Figure 9 **Average hourly aggregate system load for each month, from January ('1') to December ('12')**

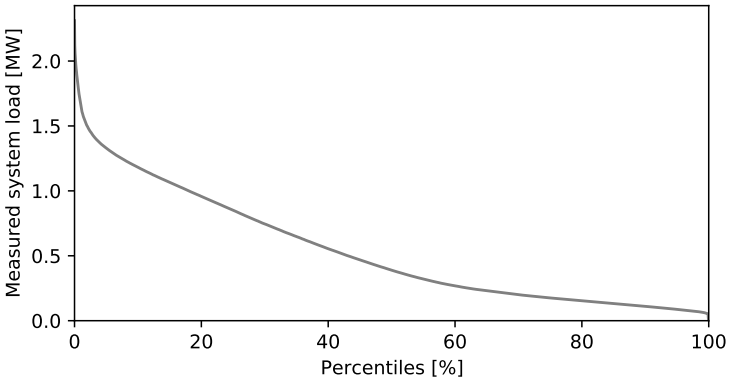

Figure 10 **Load duration curve over the year 2016**

Fig. 10 shows the load duration curve of the system for the whole year, i.e. for what share of the time a certain load level or higher is reached.

Table 7 illustrates to which extent house-specific parameters explain the electricity bills under a fixed retail rate (benchmark scenario). We find that bills are driven by the floor area, comfort preference, thermal characteristics, and gas versus electricity-based heating.

	Dependent variable:
	(1)
const	2762.033***
	(148.145)
floor_area	0.072***
	(0.002)
α	491943.471***
	(22039.625)
β	-2886.618***
	(157.644)
GAS	-44.094***
	(3.372)
Observations	437
R^2	0.903
Adjusted R^2	0.902
Residual Std. Error	25.647(df = 432)
F Statistic	1002.101*** (df = 4.0; 432.0)
Note:	*p<0.1; **p<0.05; ***p<0.01

Table 7 OLS regression results: Determinants of electricity bills under a fixed retail rate

Appendix D: Detailed Results for Case Study

Figure 11 Deviations of physical dispatch from market result (December 19-25, 2016)

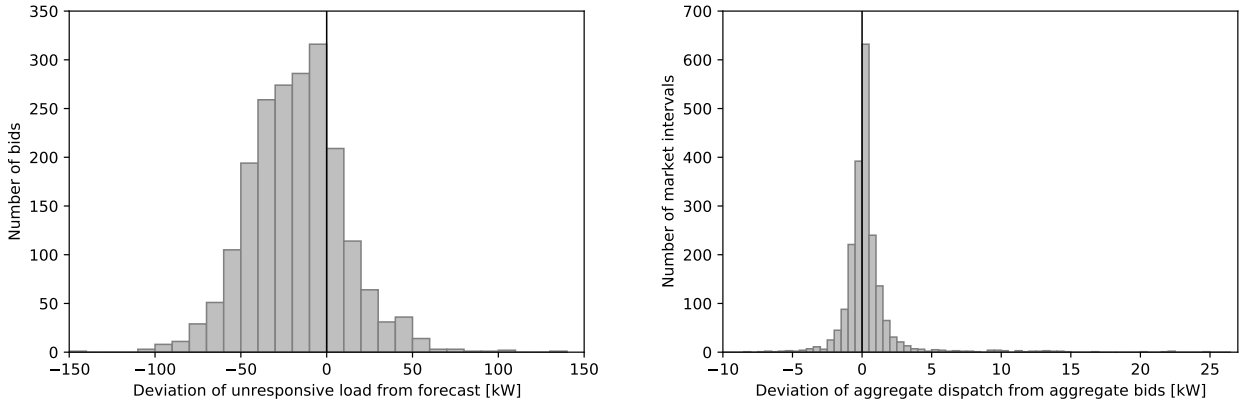

(a) Distribution of forecast errors of unresponsive load

(b) Distribution of aggregate bid deviations

Fig. 11a illustrates the retailer's forecasting errors with regard to the unresponsive load. The unresponsive load covers the base load of customers as well as grid losses. Fig. 11a shows that the actual unresponsive load tends to be over-estimated. The maximum absolute deviation is 141 kW. Furthermore, system imbalances can occur if the actual dispatch

of flexible appliances deviate from the bid submitted to the operator of the demand management system. Fig. 11b shows the distribution of such deviations, aggregated over all customers within a market interval. While deviations exist, they are distributed close to zero, with a maximum net deviation of 25 kW. This is much less than the error introduced by the unresponsive load forecast and suggests that potential deviations are not or only slightly correlated across devices.

Figure 12 Consumer surplus changes attributed to comfort change

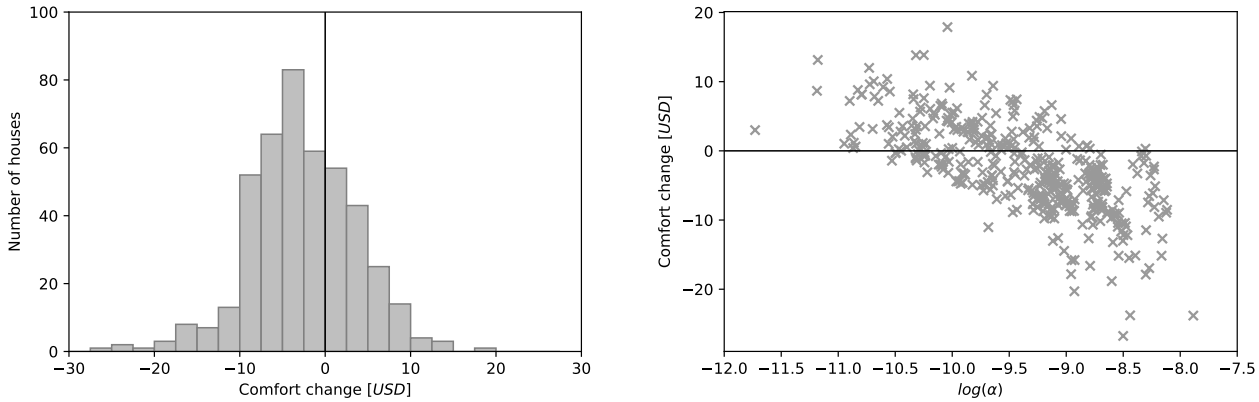

(a) Histogram of comfort changes by household

(b) House-wise comfort changes by comfort parameter

Fig. 12a displays the distribution of consumer surplus changes attributed to internal temperature changes, i.e. comfort changes. This is detailed by Fig. 12b which additionally shows the comfort change as a function of the comfort preference α. While households with a low comfort preference largely experience positive comfort changes, we observe a deterioration in comfort for households with high comfort preferences. Despite only small temperature changes as indicated by Fig. 6a, such households evaluate these deviations particularly negatively.

Figure 13 Distribution of total consumer surplus changes

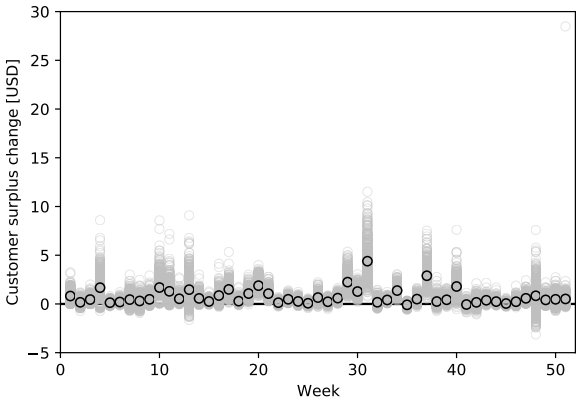

Fig. 13 further disentangles the consumer surplus changes for each week. Each grey circle represents an individual house during a specific week, the black circle represents the mean consumer surplus change. We find that changes differ throughout the year but can be high for some weeks and some customers. The minimum individual value within a week is -3.12 USD, the maximum value 28.48 USD.

	Dependent variable:	
	(1)	(2)
const	1.573	12.018***
	(1.043)	(2.151)
fixed_cost_HVAC	0.184***	0.173***
	(0.004)	(0.003)
share_unresp		0.277***
		(0.012)
corr_HVAC_WS		-168.208***
		(25.300)
GAS		-5.867***
		(0.858)
Observations	437	437
R^2	0.794	0.923
Adjusted R^2	0.794	0.923
Residual Std. Error	7.683(df = 435)	4.707(df = 432)
F Statistic	1681.540*** (df = 1.0; 435.0)	1301.690*** (df = 4.0; 432.0)
Note:		*p<0.1; **p<0.05; ***p<0.01

Table 8 OLS regression results: Determinants of absolute electricity bill savings under demand management

Table 8 illustrates to which extent house-specific parameters explain the electricity bill savings when houses participate in demand management. We find that initial bills under a fixed retail rate explain 79% of the variance in savings, i.e. households which had large bills in the first place tend to save more. Additional significant factors are the share of unresponsive load, the correlation of HVAC dispatch and WS prices in the benchmark scenario, and the existence of an electric heating system.

References

Ableitner L, Tiefenbeck V, Meeuw A, Wörner A, Fleisch E, Wortmann F (2020) User behavior in a real-world peer-to-peer electricity market. *Applied Energy* 270(2020):115061.

Adelman D, Uçkun C (2019) Crosscutting Areas—Dynamic Electricity Pricing to Smart Homes. *Operations Research* 67(6):1520–1542.

Allcott H (2011) Rethinking real-time electricity pricing. *Resource and Energy Economics* 33(4):820–842.

Astier N, Rajagopal R (2021) What Kinds of Distributed Generation Technologies Defer Network Expansions? Evidence from France. *Working Paper, Program on Energy and Sustainable Development* .

Baake P, Schwenen S, von Hirschhausen C (2020) Local Power Markets. *SSRN Electronic Journal* URL `http://dx.doi.org/10.2139/ssrn.3711353`.

Bollinger BK, Hartmann WR (2020) Information vs. Automation and implications for dynamic pricing. *Management Science* 66(1):290–314.

Borenstein S (2005) The Long-Run Efficiency of Real Time Electricity Pricing. *The Energy Journal* 26(3):93–116.

Borenstein S (2007) Customer risk from real-time retail electricity pricing: Bill volatility and hedgability. *Energy Journal* 28(2):111–130.

Borenstein S, Holland S (2005) On the Efficiency of Competitive Electricity Markets with Time-Invariant Retail Prices. *The RAND Journal of Economics* 36(3):469–493.

Burger S, Knittel CR, Pérez-Arriaga IJ, Schneider I, vom Scheidt F (2019) The Efficiency and Distributional Effects of Alternative Residential Electricity Rate Designs. *NBER Working Paper Series* (25570).

Burkhardt J, Gillingham K, Kopalle PK (2019) Experimental Evidence on the Effect of Information and Pricing on Residential Electricity Consumption. *NBER Working Paper Series* (25576).

CAISO (2017) Transmission Economic Assessment Methodology (TEAM). Technical report.

CAISO (2020) Resource Adequacy. URL `https://www.cpuc.ca.gov/ra/`, last access on 2020-07-04.

Chen N, Gallego G (2019) Welfare analysis of dynamic pricing. *Management Science* 65(1):139–151.

Chen Y, Cramton P, List JA, Ockenfels A (2020) Market Design, Human Behavior, and Management. *Management Science* (Articles in Advance).

Cohen MA, Callaway DS (2016) Effects of distributed PV generation on California's distribution system, Part 1: Engineering simulations. *Solar Energy* 128:126–138.

Cohen MA, Kauzmann PA, Callaway DS (2016) Effects of distributed PV generation on California's distribution system, part 2: Economic analysis. *Solar Energy* 128:139–152.

Comello S, Reichelstein S (2019) The emergence of cost effective battery storage. *Nature Communications* 10(1):1–9.

Dimeas A, Hatziargyriou N (2005) Operation of a multiagent system for microgrid control. *IEEE Transactions on Power Systems* 20:1447 – 1455.

ENTSO-E (2018) ENTSO-E Guideline for Cost Benefit Analysis of Grid Development Projects. Technical report.

Ercot (2018) ERCOT Monthly Operational Overview: September. Technical report.

Ercot (2019) Market Prices. URL `http://www.ercot.com/mktinfo/prices`, last access on 2019-11-25.

Ercot (2020) Settlement Points List and Electrical Buses Mapping. URL `http://mis.ercot.com/misapp/GetReports.do?reportTypeId=10008&reportTitle=Settlement\%20Points\%20List\%20and\%20Electrical\%20Buses\%20Mapping&showHTMLView=&mimicKey`, last access on 2021-03-01.

Faruqui A, Sergici S (2010) Household response to dynamic pricing of electricity: A survey of 15 experiments. *Journal of Regulatory Economics* 38(2):193–225.

Graber G, Calderaro V, Mancarella P, Galdi V (2020) Two-stage stochastic sizing and packetized energy scheduling of BEV charging stations with quality of service constraints. *Applied Energy* 260(2020):114262.

Hammerstrom DJ (2007) Pacific Northwest GridWise(TM) Testbed Demonstration Projects Part I . Olympic Peninsula Project. Technical report.

Hammerstrom DJ, Corbin CD, Fernandez N, Homer JS, Makhmalbaf A, Pratt RG, Somani A, Gilbert EI, Chandler S, Shandross R (2016) Valuation of Transactive Systems. Technical report.

IEEE Power Engineering Society (2014) IEEE 123 Node Test Feeder. URL `https://site.ieee.org/pes-testfeeders/resources/`, last access on 2020-07-04.

Inc Pecan Street (2019) Pecan Street. URL `https://www.pecanstreet.org/`.

Joskow P, Tirole J (2005) Merchant Transmission Investment. *The Journal of Industrial Economics* 53(2):233–264.

Kök AG, Shang K, Yücelc S (2018) Impact of electricity pricing policies on renewable energy investments and carbon emissions. *Management Science* 64(1):131–148.

Lin Y, Barooah P, Mathieu JL (2015) Ancillary services to the grid from commercial buildings through demand scheduling and control. *Proceedings of the American Control Conference (ACC 2015)* 3007–3012.

Liu Z, Wu Q, Oren SS, Huang S, Li R, Cheng L (2018) Distribution Locational Marginal Pricing for Optimal Electric Vehicle Charging Through Chance Constrained Mixed-Integer Programming. *IEEE Transactions on Smart Grid* 9(2):644–654.

Lohmann T, Rebennack S (2017) Tailored benders decomposition for a long-term power expansion model with short-term demand response. *Management Science* 63(6):2027–2048.

Mathieu JL, Koch S, Callaway DS (2013) State estimation and control of electric loads to manage real-time energy imbalance. *IEEE Transactions on Power Systems* 28(1):430–440.

McDonnell Nieto del Rio G, Bogel-Burroughs N, Penn I (2021) His Lights Stayed on During Texas' Storm. Now He Owes $16,752 (published on Feb 20, 2021). *New York Times* URL `https://www.nytimes.com/2021/02/20/us/texas-storm-electric-bills.html`.

Mengelkamp E, Gärttner J, Weinhardt C (2018) Decentralizing energy systems through local energy markets: The LAMP-project. *Proceedings of the 2018 Multikonferenz Wirtschaftsinformatik (2018 MKWI)* 924–930.

NREL (2015) National Solar Radiation Data Base. URL `https://rredc.nrel.gov/solar/old{\_}data/nsrdb/1991-2005/tmy3/by{\_}state{\_}and{\_}city.html`, last access on 2019-12-06.

Parag Y, Sovacool BK (2016) Electricity market design for the prosumer era. *Nature Energy* 1(4).

PJM (2020) PJM Capacity Market & Demand Response Operations PJM Manual 18, Revision 45, effective as of 2020-05-28.

Radovanovic A, Ramesh A, Koningstein R, Fork D, Weber W, Kim S, Schmalzried J, Sastry J, Dikovsky M, Bozhkov K, Pinheiro E, Lebsack C, Collyer S, Somani A, Rajagopal R, Majumdar A, Qin J, Cezar G, Rivas J, El Gamal A, Gruenich D, Chu S, Kiliccote S (2016) Powernet for distributed energy resource networks. *IEEE Power and Energy Society General Meeting 2016* .

Rassa A, van Leeuwen C, Spaans R, Kok K (2019) Developing Local Energy Markets: A Holistic System Approach. *IEEE Power and Energy Magazine* 17(5):59–70.

Seddig K, Jochem P, Fichtner W (2019) Two-stage stochastic optimization for cost-minimal charging of electric vehicles at public charging stations with photovoltaics. *Applied Energy* 242(2019):769–781.

SLAC (2020) GridLAB-D. URL `https://github.com/slacgismo/gridlabd`, last access on 2020-07-04.

US Energy Information Administration (2015) Residential Energy Consumption Survey (RECS). URL `https://www.eia.gov/consumption/residential`, last access on 2020-04-18.

US Environmental Protection Agency (2001) Energy Star: Home Sealing Specification. Technical report.

Valogianni K, Ketter W, Collins J, Zhdanov D (2020) Sustainable Electric Vehicle Charging using Adaptive Pricing. *Production and Operations Management* 29(6):1550–1572.

Vrettos E, Andersson G (2016) Scheduling and Provision of Secondary Frequency Reserves by Aggregations of Commercial Buildings. *IEEE Transactions on Sustainable Energy* 7(2):850–864.

Widergren S, Somani A, Subbarao K, Marinovici C, Fuller J, Hammerstrom J, Chassin DP (2014) AEP Ohio gridSMART Demonstration Project Real-Time Pricing Demonstration Analysis Ed. PNNL.

Wolak FA (2011) Do residential customers respond to hourly prices? Evidence from a dynamic pricing experiment. *American Economic Review* 101(3):83–87.

Wörner A, Ableitner L, Meeuw A, Wortmann F, Tiefenbeck V (2019) Peer-to-peer energy trading in the real world: Market design and evaluation of the user value proposition. *40th International Conference on Information Systems (ICIS)* .